Per Tone Equalization for DMT-Based Systems

Katleen Van Acker, Geert Leus, Marc Moonen, *Member, IEEE*, Olivier van de Wiel, and Thierry Pollet

***Abstract*—An alternative receiver structure is presented for discrete multitone-based systems. The usual structure consisting of a (real) time-domain equalizer in combination with a (complex) 1-tap frequency-domain equalizer (FEQ) per tone, is modified into a structure with a (complex) multitap FEQ per tone. By solving a minimum mean-square-error problem, the signal-to-noise ratio is maximized for each individual tone. The result is a larger bit rate while complexity during data transmission is kept at the same level. Moreover, the per tone equalization is shown to have a reduced sensitivity to the synchronization delay.**

***Index Terms*—ADSL, discrete multitone, equalization.**

I. Introduction

DISCRETE multitone (DMT) modulation has become an important transmission method, for instance, for asymmetric digital subscriber line (ADSL) which provides a high bit rate downstream channel and a lower bit rate upstream channel over twisted pair copper wire. DMT divides the available bandwidth into parallel subchannels or tones [1]. The incoming serial bitstream is divided into parallel streams, which are used to QAM-modulate the different tones. After modulation with an inverse fast Fourier transform (IFFT), a cyclic prefix is added to each symbol. If the prefix is longer than the channel impulse response, demodulation can be implemented by means of an FFT, followed by a (complex) 1-tap frequency-domain equalizer (FEQ) per tone to compensate for the channel amplitude and phase effects. A long prefix however results in a large overhead with respect to the data rate. An existing solution for this problem is to insert a (real) T-tap time-domain equalizer (TEQ) before demodulation, to shorten the channel impulse response. Imperfectly shortened channel impulse responses give rise to intersymbol interference (ISI) between two successive symbols and intercarrier interference (ICI) between different carriers [2].

Many algorithms have been developed to initialize the TEQ [3]–[7]. The TEQ-initialization of [6] computes a TEQ such that the cascade of channel impulse response and TEQ forms a finite impulse response (FIR) channel with a length shorter than the cyclic prefix. This criterion leads to a minimum mean-square-error (MMSE) problem without a direct relation to the resulting capacity of the system and has two main disadvantages. First, the resulting capacity is not a smooth function of the synchronization delay (see below). Hence, an optimal synchronization delay is not easily selected beforehand and an exhaustive search over a large range of delays is needed. Second, the resulting capacity (for a particular synchronization delay) is not necessarily the highest achievable capacity of the system. A general disadvantage, independent of the used criterion, is that the TEQ equalizes all tones "in a combined fashion" and as a result limits performance of the system. We aim at improving upon the TEQ performance by changing the receiver structure, while keeping complexity at the same level. Equalization is then done for each tone separately after the FFT-demodulation with a T-tap per tone equalizer. This enables us to implement true signal-to-noise ratio (SNR) optimization per tone, because the equalization of one carrier is totally independent of the equalization of other carriers, and results in much smoother capacity functions. More about synchronization in DMT-based systems can be found in [8].

A groupband data modem based on the orthogonally multiplexed QAM technique, using per channel equalizers [9] is proposed in [10]. These equalizers also work in the frequency domain, but they are double sampling with respect to the symbol rate and there is no cyclic prefix involved in the system. In [11], multiple-input multiple-output (MIMO) equalizers are developed for multitone systems without cyclic prefix. These equalizers are fractionally spaced with respect to the symbol rate. The per tone equalization structure we propose is based on transferring the TEQ-operations to the frequency domain. In this way, one obtains an equalizer per tone which has as its inputs T successive FFTs (i.e., at sample rate) per symbol period, which can be calculated efficiently, see Section III. The cyclic prefix remains in the system.

This paper is organized as follows. The data model of the received signal is described in Section II. In Section III, per tone equalization of DMT systems is introduced. Section IV compares the complexity of TEQ and per tone based equalization during data transmission. Section V describes the equalizer initialization. Finally simulation results are presented in Section VI.

II. Data Model

The following notation is adopted in the description of the DMT system. N is the symbol size expressed in samples, k the time index of a symbol, $X_i^{(k)}$ is a complex subsymbol for tone i ($i = 1 \cdots N$) to be transmitted at symbol period k,

Paper approved by N. C. Beaulieu, the Editor for Wireless Communication Theory of the IEEE Communications Society. Manuscript received July 6, 1999; revised December 23, 1999 and May 20, 2000. The work of G. Leus was supported by F.W.O. Flanders. This work was supported in part by Alcatel. This paper was presented in part at the Asilomar Conference on Signals, Systems and Computers, Pacific Grove, CA, October 1999, and at the Global Telecommunications Conferece (GLOBECOM'99), Rio de Janeiro, Brazil, December 1999.

K. Van Acker, G. Leus, and M. Moonen are with Katholieke Universiteit Leuven–ESAT-SISTA, 3001 Leuven, Belgium (e-mail: katleen.vanacker@esat.kuleuven.ac.be; geert.leus@esat.kuleuven.ac.be; marc.moonen@esat.kuleuven. ac.be).

O. van de Wiel and T. Pollet are with Access to Networks, Corporate Research Center, ALCATEL, 2018 Antwerpen, Belgium (e-mail: olivier.vandewiel@etsi.fr; thierry.pollet@alcatel.be).

Publisher Item Identifier S 0090-6778(01)00265-3.

0090–6778/01$10.00 © 2001 IEEE

$Y_i^{(k)}$ the demodulated output for tone i (after the FFT) and $Z_i^{(k)}$ the final output (after frequency-domain equalization). Note that $X_i^{(k)} = X_{N-(i-2)}^{*(k)} i = 2 \cdots (N/2)$ and that similar equations hold for $Y_i^{(k)}$. Further, ν denotes the length of the cyclic prefix, $s = N + \nu$ the length of a symbol including prefix, $\mathbf{h} = [h_L \cdots h_0 \cdots h_{-K}]$ the channel impulse response in reverse order, n_l additive channel noise, and y_l the received signal with l being the sample index.

To describe the data model, we consider three successive symbols[1] $X_{1:N}^{(c)}$ to be transmitted at $c = k-1, k, k+1$, respectively. The kth symbol is the symbol of interest, the previous and the next symbol are used to include interferences with neighboring symbols in our model. The received signal may then be specified as follows:

$$\overbrace{\begin{bmatrix} y_{k\cdot s+\nu-T+2+\delta} \\ \ddots \\ y_{(k+1)\cdot s+\delta} \end{bmatrix}}^{\mathbf{y}} = \left[\begin{array}{c|c|c} \mathbf{O}_{(1)} & \begin{array}{ccc} \boxed{\mathbf{h}} & 0 & \cdots \\ & \ddots & \\ 0 & \cdots & \boxed{\mathbf{h}} \end{array} & \mathbf{O}_2 \end{array}\right] \cdot \begin{bmatrix} \mathbf{P} & \mathbf{O} & \mathbf{O} \\ \mathbf{O} & \mathbf{P} & \mathbf{O} \\ \mathbf{O} & \mathbf{O} & \mathbf{P} \end{bmatrix}$$
$$\cdot \begin{bmatrix} \mathcal{I}_N & \mathbf{O} & \mathbf{O} \\ \mathbf{O} & \mathcal{I}_N & \mathbf{O} \\ \mathbf{O} & \mathbf{O} & \mathcal{I}_N \end{bmatrix} \cdot \overbrace{\begin{bmatrix} X_{1:N}^{(k-1)} \\ X_{1:N}^{(k)} \\ X_{1:N}^{(k+1)} \end{bmatrix}}^{\mathbf{X}} + \overbrace{\begin{bmatrix} n_{k\cdot s+\nu-T+2+\delta} \\ \vdots \\ n_{(k+1)\cdot s+\delta} \end{bmatrix}}^{\mathbf{n}}$$
$$= \mathbf{H} \cdot \mathbf{X} + \mathbf{n} \tag{1}$$

$\mathbf{O}_{(1)}$ and $\mathbf{O}_{(2)}$ are zero matrices of size $(N+T-1) \times (N+\nu-T+1-L+\nu+\delta)$ and $(N+T-1) \times (N+\nu-K-\delta)$, respectively.

$$\mathbf{P} = \left[\begin{array}{c|c} \mathbf{O} & \mathbf{I}_\nu \\ \hline \multicolumn{2}{c}{\mathbf{I}_N} \end{array}\right]$$

adds the cyclic prefix. The $\mathcal{I}_N$ matrices are $N \times N$ IFFT matrices and modulate the input symbols. The zero reference delay corresponds to the head $[h_{-K} \cdots h_{-1}]$ and the tail $[h_{\nu+1} \cdots h_L]$ which maximize the energy in $[h_0 \cdots h_\nu]$. δ is the synchronization delay, and is a design parameter.[2]

III. Per Tone Equalization in a DMT Modem

Different receivers will be represented as signal flow graphs (SFGs), building blocks of which are given in Fig. 1. The standard receiver with TEQ [3]–[7] is shown in Fig. 2. This receiver is based on the following operation:

$$\begin{bmatrix} Z_1^{(k)} \\ \vdots \\ Z_N^{(k)} \end{bmatrix} = \begin{bmatrix} D_1 & 0 & \cdots \\ 0 & \ddots & 0 \\ \vdots & 0 & D_N \end{bmatrix} \cdot \overbrace{\mathcal{F}_N \cdot (\mathbf{Y} \cdot \mathbf{w})}^{1\,\text{FFT}} \tag{2}$$

[1] $X_{1:N}^{(c)}$ denotes vector $[X_1^{(c)} \cdots X_N^{(c)}]^{\mathrm{T}}$.

[2] The synchronization delay, discussed in this paper, corresponds to the alignment of the symbols. So, it determines which $N + \nu$ received samples belong to the same received symbol.

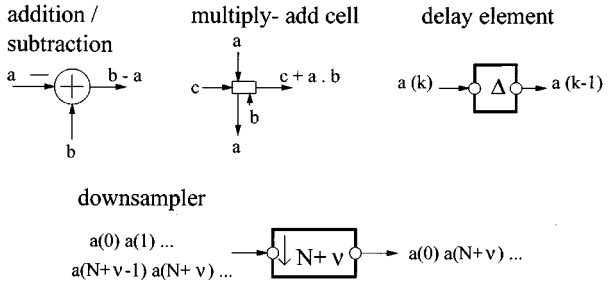

Fig. 1. Signal flow graph building blocks.

where

$$\mathbf{Y} = \begin{bmatrix} y_{k\cdot s+\nu+1} & y_{k\cdot s+\nu} & \cdots & y_{k\cdot s+\nu-T+2} \\ y_{k\cdot s+\nu+2} & y_{k\cdot s+\nu+1} & \cdots & y_{k\cdot s+\nu-T+3} \\ & \ddots & \ddots & \\ y_{(k+1)\cdot s} & y_{(k+1)\cdot s-1} & \cdots & y_{(k+1)\cdot s-T+1} \end{bmatrix} \tag{3}$$

and $\mathbf{w}_{T\times 1} = [w_0 w_1 \cdots w_{T-1}]^{\mathrm{T}}$ is the (real) T-tap TEQ, $\mathcal{F}_N$ an $N \times N$ FFT-matrix, D_i the (complex) 1-tap FEQ for tone i, and $\mathbf{Y}$ an $N \times T$ Toeplitz matrix[3] which contains exactly the same received signal samples as vector $\mathbf{y}$ in (1). For the sake of compact notation, the synchronization delay δ is omitted in $\mathbf{Y}$.

Our approach is based on transferring the TEQ-operations to the frequency domain (i.e., after the FFT-demodulation). For a single tone i, we can rewrite the above operations as follows:

$$Z_i^{(k)} = D_i \cdot \mathrm{row}_i(\mathcal{F}_N) \cdot (\mathbf{Y} \cdot \mathbf{w}) = \mathrm{row}_i \underbrace{(\mathcal{F}_N \cdot \mathbf{Y})}_{T\,\text{FFTs}} \cdot \underbrace{\mathbf{w} \cdot D_i}_{\mathbf{w}_i}. \tag{4}$$

By putting D_i to the right, one has $\mathbf{w} \cdot D_i = (\mathbf{w}_i)_{T\times 1}$ which is a (complex) T-tap FEQ for tone i. The next step then is to allow each tone to have its own optimal TEQ, (be it) implemented as a T-tap FEQ $\mathbf{w}_i$. The corresponding receiver structure is shown in Fig. 3. From (4), it follows that the latency of the system is the same for the TEQ-approach as for the per tone equalization.

Note that, as indicated in (4), instead of one FFT-operation per symbol, we now apparently need T FFT-operations (one FFT for each column of $\mathbf{Y}$). Fortunately, because of the Toeplitz structure of $\mathbf{Y}$, these FFTs can be calculated efficiently by means of a sliding FFT [12]. Only one "full" FFT has to be calculated (for the first column of $\mathbf{Y}$) and the $T-1$ remaining FFTs can be deduced as follows, as is proven in Appendix A:

$$\begin{aligned} &(\mathcal{F}_N \cdot \mathbf{Y}(:, m+1)) \\ &\quad = (\mathcal{F}_N \cdot \mathbf{Y}(:, m)) \odot \mathbf{p} \\ &\qquad + \begin{bmatrix} 1 \\ \vdots \\ 1 \end{bmatrix}_{N\times 1} \cdot \left(y_{k\cdot s+\nu-(m-1)} - y_{k\cdot s+s-(m-1)}\right) \\ &\mathbf{p}^{\mathrm{T}} = [\alpha^0 \quad \alpha^1 \quad \cdots \quad \alpha^{N-1}] \quad \alpha = e^{-j2\pi(1/N)} \end{aligned} \tag{5}$$

[3] The capital boldface letter $\mathbf{Y}$ is a matrix of received signal samples. The capital letter $Y_i^{(k)}$ (the demodulated output for tone i at symbol period k) is a complex subsymbol.

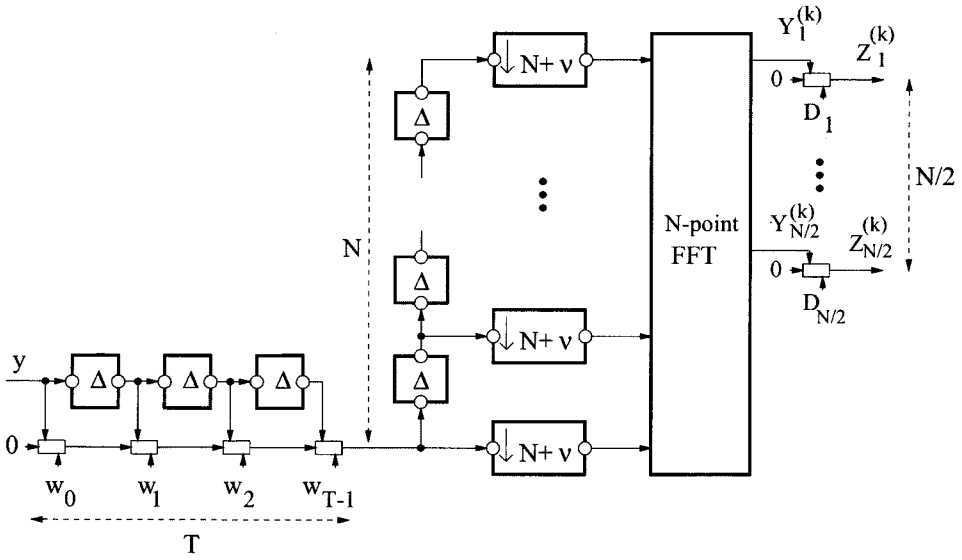

Fig. 2. T-tap TEQ with 1-tap FEQ per tone.

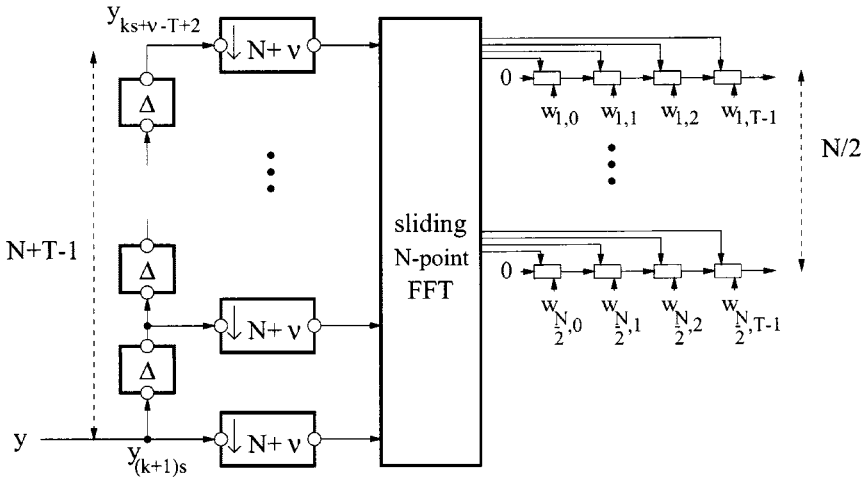

Fig. 3. T-tap FEQ per tone.

where $m = 1 \cdots T-1$. The $\odot$ represents a componentwise multiplication. $\mathbf{Y}(:, m+1)$ is the $(m+1)$th column of $\mathbf{Y}$, and $y_{k\cdot s+\nu-(m-1)}$ is its first element. $\mathbf{Y}(:, m)$ is the mth column of $\mathbf{Y}$, and $y_{k\cdot s+s-(m-1)}$ is its last element. For tone i, all relevant FFT-elements can thus be derived as linear combinations of the ith component of the FFT of the first column of $\mathbf{Y}$ and $T-1$ difference terms $y_{k\cdot s+\nu-(m-1)} - y_{k\cdot s+s-(m-1)}$ for $m = 1 \cdots T-1$.

To reduce complexity even further, these linear combinations can then be incorporated in the FEQ coefficients such that the global FEQ for each tone i has as its inputs the ith output of the FFT and $T-1$ (real) difference terms (see Fig. 4). The modified per tone equalizers are denoted as $\mathbf{v}_i = [v_{i,0} \cdots v_{i,T-1}]^{\mathrm{T}}$ and can be calculated from the original FEQs $\mathbf{w}_i$ as follows:

$$\begin{bmatrix} v_{i,0} \\ v_{i,1} \\ \vdots \\ v_{i,T-1} \end{bmatrix} = \begin{bmatrix} 1 & \alpha^{i-1} & \cdots & \alpha^{(i-1)(T-1)} \\ 0 & 1 & \ddots & \ddots \\ \vdots & \ddots & \ddots & \alpha^{i-1} \\ 0 & \cdots & 0 & 1 \end{bmatrix} \cdot \begin{bmatrix} w_{i,0} \\ w_{i,1} \\ \vdots \\ w_{i,T-1} \end{bmatrix} \tag{6}$$

which is proven in Appendix B. This can be calculated efficiently by the recursion formula

$$v_{i,t+1} \cdot \alpha^{i-1} + w_{i,t} = v_{i,t} \tag{7}$$

for tone $i = 1 \cdots N$ with $t = 0 \cdots T-2$, $v_{i,T-1} = w_{i,T-1}$, and $\alpha = e^{-j2\pi(1/N)}$ (see also Appendix B). SFGs of the recursion are presented in Fig. 5 for transformation from $\mathbf{v}_i$ to $\mathbf{w}_i$ and vice versa. These transformations are important when grouping tones, because the equalizer $\mathbf{v}_i$ has two functions, it equalizes the channel for tone i and includes the sliding Fourier transform corresponding to tone i. This equalizer cannot be used as such for other tones in the same group. The equalizer $\mathbf{w}_i$ on the other hand, can be used as such for other tones of the same group, because this equalizer does not include the sliding Fourier transform for tone i (see Section V-B).

As indicated in Fig. 4, the per tone equalization structure works with the $\mathbf{v}_i$'s, while the $\mathbf{w}_i$'s are not computed explicitly (except when tone grouping is used, then the $\mathbf{w}_i$'s are computed for the center tones). The advantages of the per tone ap-

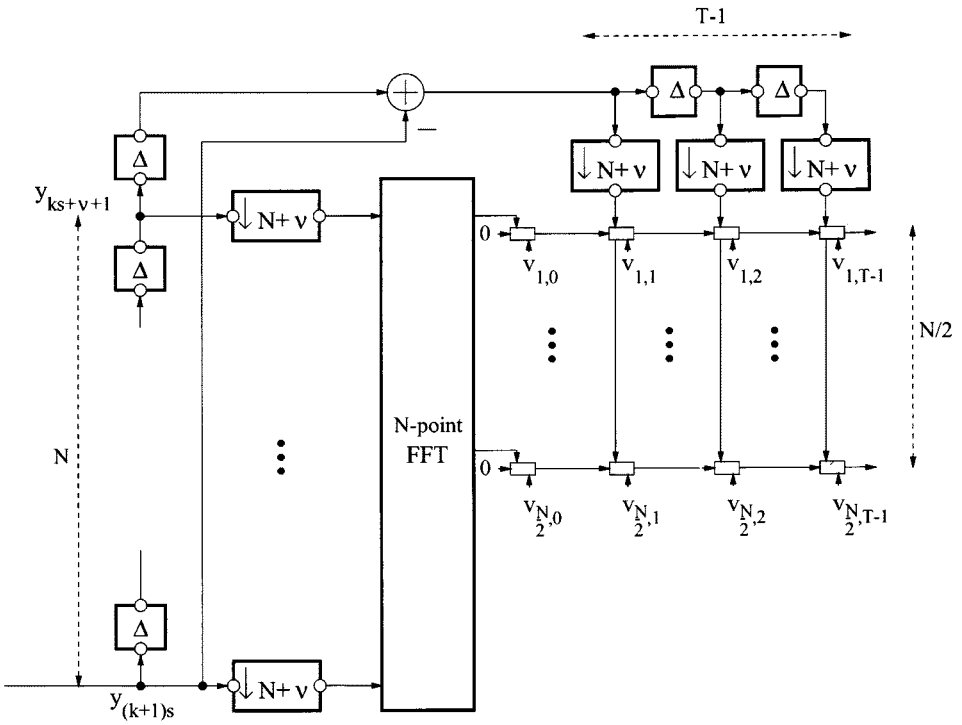

Fig. 4. Modified T-tap FEQ per tone.

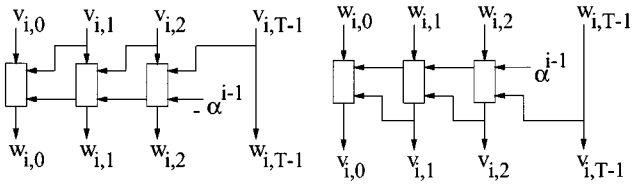

Fig. 5. Recursions $\mathbf{v}_i$ to $\mathbf{w}_i$ and $\mathbf{w}_i$ to $\mathbf{v}_i$.

proach over the usual TEQ approach will be demonstrated in Section VI.

IV. Complexity During Data Transmission

Because the per tone equalizers work at a downsampled rate with respect to the TEQ, the total complexity of the TEQ-based structure and the modified per tone equalizer-based structure is easily shown to be roughly equal for a particular T and N.

Complexity calculations for equalization consisting of TEQ and 1-tap FEQ per tone are presented in Table I. F_s is the sample frequency and $(N+\nu)/F_s$ the symbol duration. N_u denotes the number of used tones. The last row of the table is an approximation where the number of used tones is taken $N_u = N/2$ and the symbol duration is N/F_s.

The complexity of the per tone equalization with FEQs $\mathbf{v}_i$ is presented in Table II. A cartesian representation of the complex numbers is used. The different terms in the third row (FEQ) correspond to the complexities of the following operations: product of complex input with complex tap, $T-1$ products of real input with complex tap, sum of T complex tap outputs and calculation of $T-1$ difference terms. In the last row, similar approximations are used as in Table I.

TABLE I
Complexity of Equalization with TEQ and 1-Tap FEQ per Tone

	# multiplications	# additions
TEQ	F_sT	$F_s(T-1)$
FFT	$\frac{F_s}{N+\nu}\mathcal{O}(N\cdot\log(N))$	$\frac{F_s}{N+\nu}\mathcal{O}(N\cdot\log(N))$
FEQ Polar representation	$N_u\frac{F_s}{N+\nu}$	$N_u\frac{F_s}{N+\nu}$
TEQ + FEQ	$F_s(T+\frac{N_u}{N+\nu})$	$F_s(T-1+\frac{N_u}{N+\nu})$
approximation	$F_s(T+\frac{1}{2})$	$F_s(T-\frac{1}{2})$

TABLE II
Complexity of per Tone Equalizers

	# multiplications	# additions
TEQ		
FFT	$\frac{F_s}{N+\nu}\mathcal{O}(N\cdot\log(N))$	$\frac{F_s}{N+\nu}\mathcal{O}(N\cdot\log(N))$
FEQ Cartesian representation	$\frac{F_s}{N+\nu}N_u[4+2(T-1)]$ $=2\frac{F_s}{N+\nu}N_u(T+1)$	$\frac{F_s}{N+\nu}N_u[2+2(T-1)]$ $+\frac{F_s}{N+\nu}(T-1)$ $=\frac{F_s}{N+\nu}(2N_uT+T-1)$
approximation	$F_s(T+1)$	$F_sT+\frac{F_s}{N}(T-1)$

We can conclude that the resulting complexities are comparable and both of order F_sT. The complexity of the per tone

method can be reduced even further by varying the equalizer length per tone and setting the length to zero for nonused tones. This is not pursued in this paper.

V. Equalizer Initialization

For each of the used tones, we find the MMSE-FEQ (for a particular choice of δ) by minimizing the following cost function:

$$\begin{aligned}\min_{\mathbf{w}_i} & J(\mathbf{w}_i) \\ &= \min_{\mathbf{w}_i} \mathcal{E}\left\{\left|Z_i^{(k)} - X_i^{(k)}\right|^2\right\} \\ &= \min_{\mathbf{w}_i} \mathcal{E}\left\{\left|\overline{\mathbf{w}}_i^{\mathrm{T}} \cdot \begin{bmatrix} \boxed{\mathcal{F}_N(i,:)} & 0 & \cdots \\ & \ddots & \ddots \\ 0 & \cdots & \boxed{\mathcal{F}_N(i,:)} \end{bmatrix} \cdot \mathbf{y} - X_i^{(k)}\right|^2\right\}\end{aligned} \tag{8}$$

with vector[4] $\overline{\mathbf{w}}_i^{\mathrm{T}} = [w_{i,T-1} \cdots w_{i,0}]$ and $\mathcal{F}_N(i,:)$ the ith row of $\mathcal{F}_N$. This MMSE-FEQ thus optimizes the SNR for each tone separately.

Similarly, the modified FEQ $\mathbf{v}_i$ may be computed from

$$\begin{aligned}\min_{\mathbf{v}_i} & J(\mathbf{v}_i) \\ &= \min_{\mathbf{v}_i} \mathcal{E}\left\{\left|\overline{\mathbf{v}}_i^{\mathrm{T}} \cdot \underbrace{\left[\begin{array}{c|c|c} \mathbf{I}_{T-1} & \mathbf{O} & -\mathbf{I}_{T-1} \\ \hline \mathbf{O} & \multicolumn{2}{c}{\mathcal{F}_N(i,:)} \end{array}\right]}_{\mathbf{F}_i} \cdot \mathbf{y} - X_i^{(k)}\right|^2\right\}\end{aligned} \tag{9}$$

with $\overline{\mathbf{v}}_i^{\mathrm{T}} = [v_{i,T-1} \cdots v_{i,0}]$. The first block row in $\mathbf{F}_i$ is seen to extract the difference terms, while the last row corresponds to the single FFT.

A. Equalizer Initialization Based on Channel Models

Formula (9) may be combined with (1) resulting in an initialization formula which is applicable whenever a channel model is available, as well as signal and noise covariance matrices.[5] In the sequel, we use the following notation: $\mathbf{e}_i^{(k)} = [0 \cdots 0\,1\,0 \cdots 0]_{1\times 3N}$ with the nonzero entry in the $(N+i)$th column, $\mathbf{H}$ which includes channel convolution, adding of prefix and modulation, see equation (1), $\mathbf{R}_{\mathbf{X}} = \mathcal{E}\{\mathbf{X}\mathbf{X}^{\mathrm{H}}\}$ the autocorrelation of vector $\mathbf{X}$ and finally $\mathbf{R}_{\mathbf{n}} = \mathcal{E}\{\mathbf{n}\mathbf{n}^{\mathrm{H}}\}$ the autocorrelation of the noise $\mathbf{n}$. Combining (9) with (1) then results in

$$\begin{aligned} J(\mathbf{v}_i) &= \mathcal{E}\left\{\left|\overline{\mathbf{v}}_i^{\mathrm{T}}\mathbf{F}_i(\mathbf{H}\mathbf{X}+\mathbf{n}) - \mathbf{e}_i^{(k)}\mathbf{X}\right|^2\right\} \\ &= \mathcal{E}\left\{\left|\begin{bmatrix}\mathbf{X}^{\mathrm{H}} & \mathbf{n}^{\mathrm{H}}\end{bmatrix} \cdot \begin{bmatrix}\mathbf{H}^{\mathrm{H}}\mathbf{F}_i^{\mathrm{H}}\overline{\mathbf{v}}_i^* - \mathbf{e}_i^{(k)\mathrm{H}} \\ \mathbf{F}_i^{\mathrm{H}}\overline{\mathbf{v}}_i^*\end{bmatrix}\right|^2\right\} \\ &= \left\|\begin{bmatrix}\mathbf{R}_{\mathbf{X}}^{1/2} & \mathbf{O} \\ \mathbf{O} & \mathbf{R}_{\mathbf{n}}^{1/2}\end{bmatrix} \cdot \begin{bmatrix}\mathbf{H}^{\mathrm{H}}\mathbf{F}_i^{\mathrm{H}}\overline{\mathbf{v}}_i^* - \mathbf{e}_i^{(k)\mathrm{H}} \\ \mathbf{F}_i^{\mathrm{H}}\overline{\mathbf{v}}_i^*\end{bmatrix}\right\|_2^2 \\ &= \left\|\underbrace{\begin{bmatrix}\mathbf{R}_{\mathbf{X}}^{1/2}\mathbf{H}^{\mathrm{H}}\mathbf{F}_i^{\mathrm{H}} \\ \mathbf{R}_{\mathbf{n}}^{1/2}\mathbf{F}_i^{\mathrm{H}}\end{bmatrix}}_{\mathbf{U}}\overline{\mathbf{v}}_i^* - \underbrace{\begin{bmatrix}\mathbf{R}_{\mathbf{X}}^{1/2}\mathbf{e}_i^{(k)\mathrm{H}} \\ \mathbf{0}\end{bmatrix}}_{\mathbf{d}}\right\|_2^2. \end{aligned} \tag{10}$$

This least squares problem (for a particular choice of δ) is then solved for each tone i, for instance by a QR decomposition [13] of the compound matrix $[\mathbf{U}\,\mathbf{d}]$. The resulting signal, ISI–ICI and noise energy for tone i can then be found, respectively, as

$$S_i = \left|\left(\mathbf{R}_{\mathbf{X}}^{1/2}\mathbf{H}^{\mathrm{H}}\mathbf{F}_i^{\mathrm{H}}\right)_{(N+i,:)}\overline{\mathbf{v}}_i^*\right|^2 \tag{11}$$

$$I_i = \left\|\mathbf{R}_{\mathbf{X}}^{1/2}\mathbf{H}^{\mathrm{H}}\mathbf{F}_i^{\mathrm{H}}\overline{\mathbf{v}}_i^*\right\|^2 - S_i \tag{12}$$

$$N_i = \left\|\mathbf{R}_{\mathbf{n}}^{1/2}\mathbf{F}_i^{\mathrm{H}}\overline{\mathbf{v}}_i^*\right\|^2. \tag{13}$$

The SNR of tone i becomes $\mathrm{SNR}_i = (S_i/(I_i+N_i))$.

B. Tone Grouping

To reduce initialization complexity, we can combine tones into groups. For each group, only one set of equalizer coefficients ($\mathbf{v}_{i_1}$ for tone i_1) is computed. Then the corresponding $\mathbf{w}_{i_1}$ is computed from $\mathbf{v}_{i_1}$, by making use of (7). The $\mathbf{v}_{i_2}$'s for the remaining tones in the same group are then defined as (see Fig. 5)

$$v_{i_2,t+1}\cdot\alpha^{i_2-1} + w_{i_1,t} = v_{i_2,t}. \tag{14}$$

The overall equalizer for tone i_2 is then $D_{i_2}\cdot[v_{i_2,0}\cdots v_{i_2,T-1}]$ where D_{i_2} is an additional 1-tap FEQ for tone i_2, similar to the 1-tap FEQ in the TEQ-based implementation, see Section III. Simulations show that combining tones into groups of e.g., 11 tones, does not reduce performance significantly, see Section VI, while the initialization complexity is reduced roughly by a factor 11.

The complexity during data transmission does not decrease by tone grouping because one equalizer $\mathbf{v}_i$ is still needed for each tone i.

VI. Simulation Results

A. Per Tone Equalization

In Fig. 6 some ADSL simulation results are presented for downstream to compare the different equalizers. Standard channel [14] T1.601-#9 with NEXT from 12 DSL and 12 HDSL disturbances is considered. To compute capacity, we take the SNR gap $\Gamma = 9.8$ dB, noise margin $\gamma_m = 6$ dB, coding gain $\gamma_c = 3$ dB. The number of bits b assigned to tone i is

$$b_i = \left\lfloor \log_2\left(1 + 10^{((\mathrm{SNR}_i - \Gamma - \gamma_m + \gamma_c)/10)}\right)\right\rfloor. \tag{15}$$

[4] $\overline{\mathbf{w}}_i$ denotes vector $\mathbf{w}_i$ with its elements in reverse order.

[5] Alternatively (9) may be used for a training sequence based initialization of the per tone equalizers. Efficient implementation schemes for such initialization procedures will be reported elsewhere.

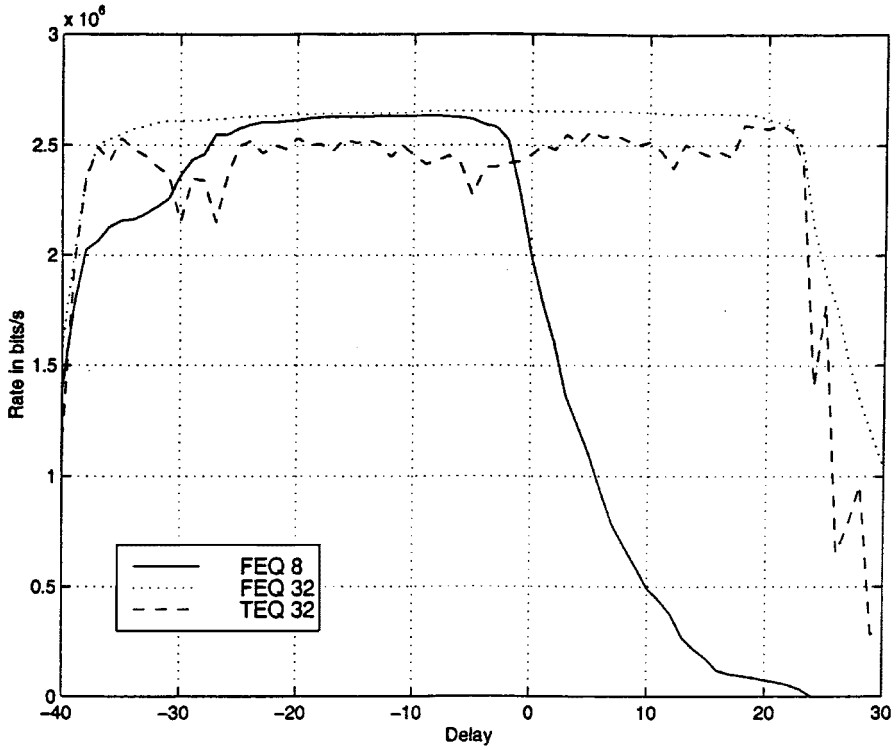

Fig. 6. Comparison of TEQ with per tone equalization for standard channel T1.601-#9 with NEXT from 12 DSL and 12 HDSL disturbances (downstream).

The rate is computed with the formula

$$rate = \left(\sum_{i=\text{used tone}} b_i \right) \cdot \frac{F_s}{N+\nu} \tag{16}$$

with $F_s = 2.208$ MHz for downstream.

When computing the covariance matrix of the input $\mathbf{R_X}$, which is assumed to be diagonal, we take into account the used tones, i.e., tone 38 up to tone 256. This "mask" is put over the diagonal of $\mathbf{R_X}$, which means that the diagonal elements corresponding to unused tones are set to zero. Other parameters are $N = 512$, $\nu = 32$, $\text{psd}_x = -40$ dBm/Hz. The dotted line gives the capacity for a 32-tap per tone structure (FEQ), as a function of the synchronization delay δ. This capacity is always higher and significantly smoother than the one given by the dashed line, for a 32-tap TEQ-based structure calculated with the time-domain channel impulse response shortening procedure of [6]. Because the capacity of the TEQ reached for different values of the delay parameter does not evolve smoothly, an optimal synchronization delay is not easily selected beforehand and an exhaustive search over a large range of delays is needed. The per tone equalization however shows a smooth behavior. Hence, selecting an appropriate synchronization delay is not so critical.

The solid line shows the capacity with eight-tap FEQs for the used tones for each delay. It is seen that for a comparable performance, one can reduce the equalizer filter length from 32 down to 8 taps. It's worth noting that shorter equalizers have a smaller delay range in which optimum capacity is achieved.

Investigation of the SNR distribution over the used tones shows that the traditional approach of computing TEQ taps causes dips in the SNR distribution whereas the per tone equalization has a smooth SNR distribution. This is demonstrated in Figs. 7–9 where the SNR is plotted over the used tones for the (relative) delay range $[-40:5:30]$, i.e., from delay -40 to delay 30 in steps of 5. Equalization of one tone is now independent of equalization of all the other tones. Hence, the equalization effort may be concentrated on the most affected tones by adjusting T for each tone. This is especially interesting when radio frequency interference is present. Longer equalizers in the neighborhood of the interferer improve performance of the system without drastic complexity increase. Another advantage is the fact that no effort is wasted on the equalization of unused tones, which corresponds to an extra complexity saving.

B. Tone Grouping

In Figs. 10 and 11, different equalization schemes for the same channel are compared, respectively, for $T = 8$ and $T = 32$. For each of these lengths, the bit rate is calculated for the "full" per tone equalization, for equalization with grouping of 11 tones, grouping of 51 tones and the TEQ. Grouping per 11 tones results in 20 groups, grouping per 51 tones results in 4 groups. For each group the equalizer of the central tone is used for the whole group.[6] It is clear that combining tones into groups of 11 tones does not reduce performance significantly. When more tones are combined, e.g., 51 tones, the difference with the per tone equalization turns out to be larger with larger equalizer length T.

[6]Remark that the per tone equalizer w_{i_1} is in common for such a group but that the corresponding modified per tone equalizer v_{i_2} has to be calculated with (14).

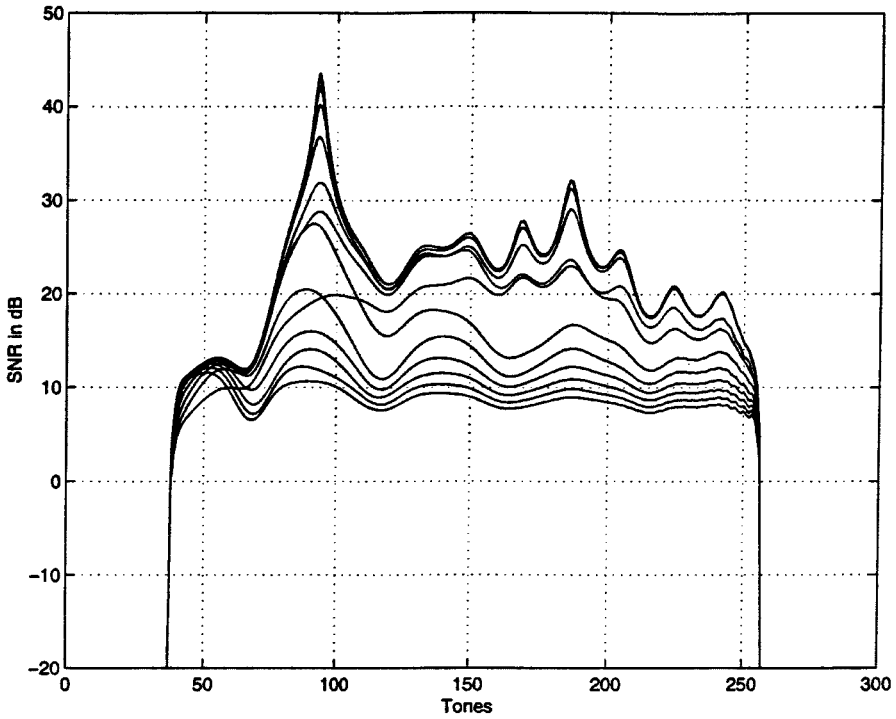

Fig. 7. SNR distribution for per tone equalization with $T = 8$ in delay range $[-40:5:30]$.

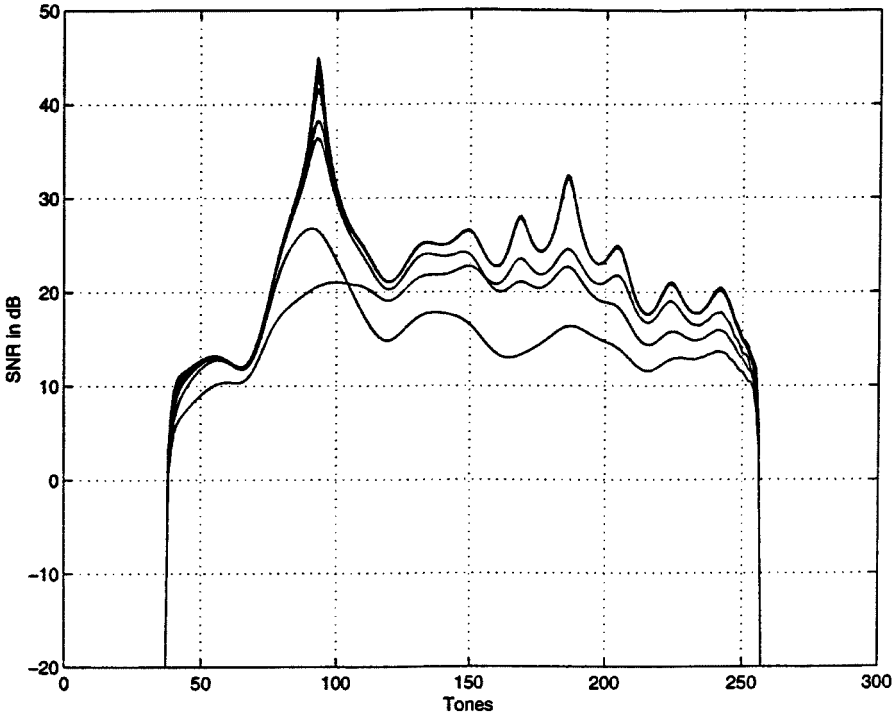

Fig. 8. SNR distribution for per tone equalization with $T = 32$ in delay range $[-40:5:30]$.

VII. Conclusions

A new equalization scheme for DMT receivers has been developed. The (real) T-tap TEQ is transferred to the frequency domain which leads to a (complex) T-tap FEQ for each tone separately. The per tone equalization structure is shown to have comparable complexity during data transmission.

The T-tap FEQ allows us to optimize the SNR and hence the bit rate for each tone. The main advantages with respect to the original structure, are reduced sensitivity to the synchronization delay and smaller equalizer size for the same performance. Furthermore equalization effort can be concentrated on the most affected tones by increasing the number of equalization filter coefficients for these tones. No effort is wasted to equalize unused carriers because there the number of taps can be set to zero.

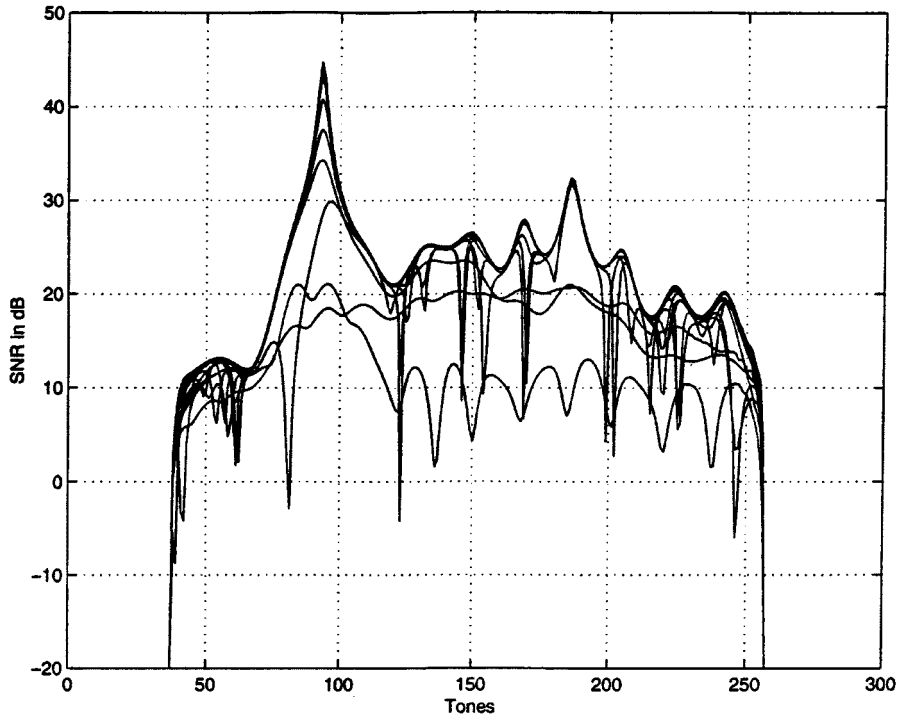

Fig. 9. SNR distribution for TEQ with $T = 32$ in delay range $[-40:5:30]$.

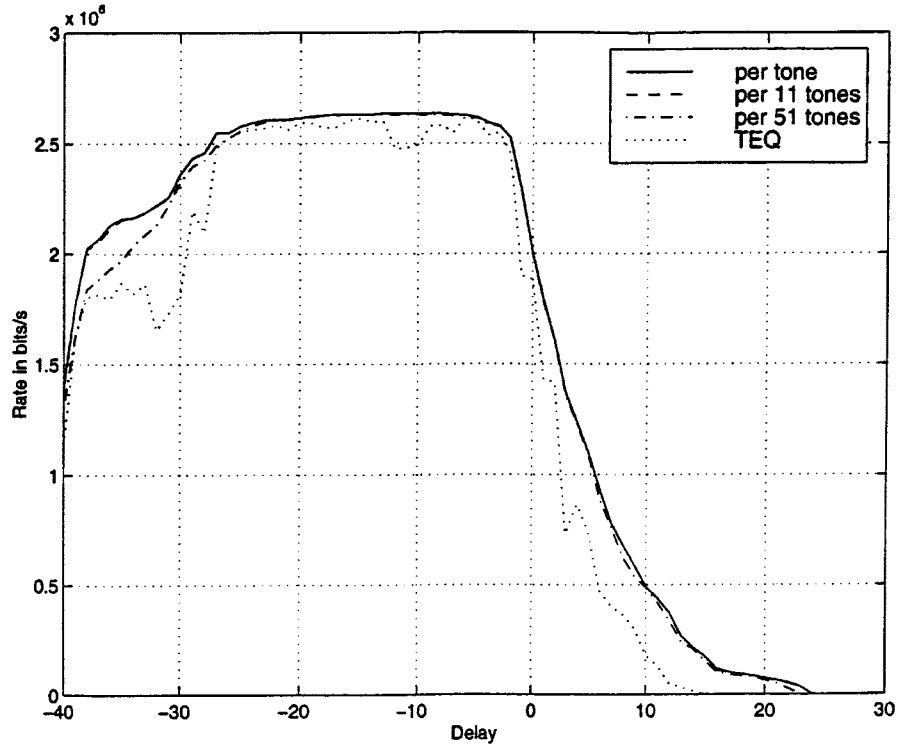

Fig. 10. Comparison of different equalization schemes for $T = 8$.

In this paper, direct initialization of the per tone equalizers is described. Efficient iterative initialization schemes will be developed in future work. Moreover initialization complexity can be reduced by combining tones. It is demonstrated that combining tones into groups of 11 tones does not reduce performance significantly.

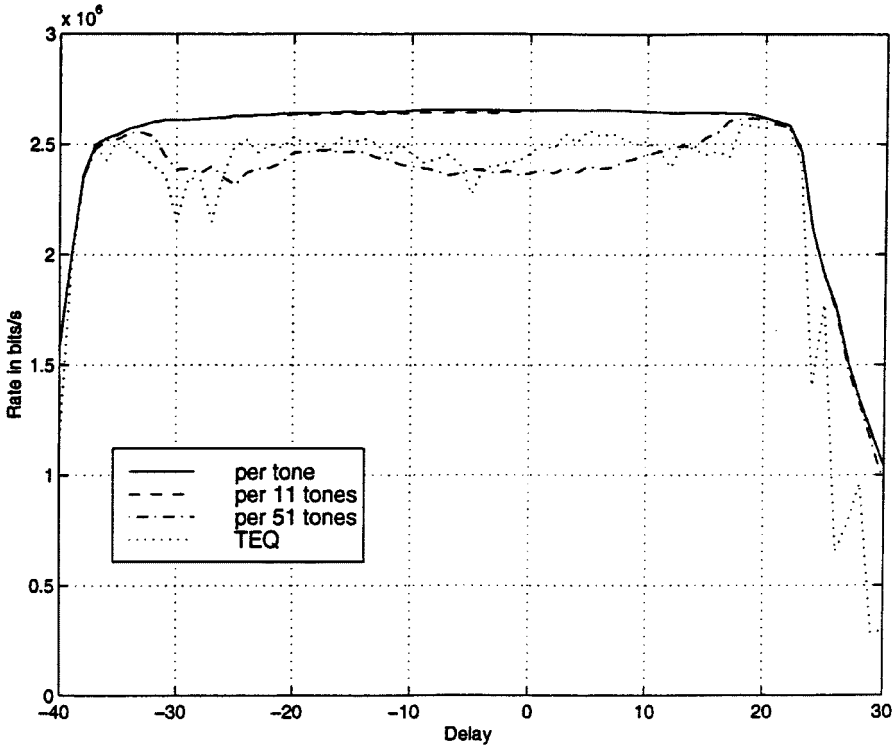

Fig. 11. Comparison of different equalization schemes for $T = 32$.

APPENDIX A

Equation (5) is proven as follows. Given two vectors: $\mathbf{a} = [a_0 a_1 \cdots a_{N-1}]$ and $\mathbf{b} = [b_0 b_1 \cdots b_{N-1}] = [\alpha a_0 a_1 \cdots a_{N-2}]$. The FFT of $\mathbf{a}$ is

$$A_{i-1} = \sum_{k=0}^{N-1} a_k e^{-j2\pi((i-1)k/N)} \tag{17}$$

where $i = 1 \cdots N$ is the tone index. The FFT of $\mathbf{b}$ is

$$B_{i-1} = \sum_{k=0}^{N-1} b_k e^{-j2\pi((i-1)k/N)} \tag{18}$$

$$= c + \sum_{k=1}^{N-1} a_{k-1} e^{-j2\pi((i-1)k/N)} \tag{19}$$

$$= c + \left(\sum_{k=0}^{N-2} a_k e^{-j2\pi((i-1)k/N)} \right) e^{-j2\pi((i-1)/N)}. \tag{20}$$

With phase $\mathbf{p}$ defined as in equation (5), one obtains

$$\mathbf{p}(i-1) = e^{-j2\pi(i-1)/N} \tag{21}$$

$$A_{i-1} \cdot \mathbf{p}(i-1) = \left(\sum_{k=0}^{N-2} a_k e^{-j2\pi((i-1)k/N)} \right) \cdot e^{-j2\pi(i-1)/N} + a_{N-1}. \tag{22}$$

By comparison of equations (20) and (22), one obtains

$$B_{i-1} = A_{i-1} \cdot \mathbf{p}(i-1) - a_{N-1} + c \quad \text{for } i = 1 \cdots N. \tag{23}$$

APPENDIX B

Equation (6) is proven as follows. Without loss of generality, we take $T = 3$ and $N = 4$. Analogous to equation (4), we write the demodulated output for the ith tone as

$$Z_i^{(k)} = \mathcal{F}_4(i, :) \cdot \begin{bmatrix} a & b & c \\ d & a & b \\ e & d & a \\ f & e & d \end{bmatrix} \cdot \mathbf{w}_i \tag{24}$$

where the matrix contains received signal samples and $\mathbf{w}_i$ is a 3×1 vector. This expression can be split into a circulant part and a correction on this part, as follows:

$$Z_i^{(k)} = \mathcal{F}_4(i,:) \cdot \left(\begin{bmatrix} a & f & e \\ d & a & f \\ e & d & a \\ f & e & d \end{bmatrix} + \begin{bmatrix} 0 & b-f & c-e \\ 0 & 0 & b-f \\ 0 & 0 & 0 \\ 0 & 0 & 0 \end{bmatrix} \right) \cdot \mathbf{w}_i. \tag{25}$$

Let A_{i-1} be $\mathcal{F}_4(i, :)$ times the first column of the circulant matrix. The $\mathcal{F}_4(i, :)$ operating on the other columns, which are circular shifts of the first column, gives rise to an additional phase. With $\alpha = e^{-j2\pi(1/N)}$ (here $N = 4$), the $\mathcal{F}_4(i, :)$ operating on the second matrix is written as a "normal" FFT-operation[7]

$$Z_i^{(k)} = A_{i-1} \cdot [1 | \alpha^{i-1} | \alpha^{(T-1)(i-1)}] \cdot \mathbf{w}_i + [0 | (b-f) | (c-e) + (b-f) \cdot \alpha^{i-1}] \cdot \mathbf{w}_i. \tag{26}$$

[7] $\mathcal{F}_N(i, :) = [1 | \alpha^{(i-1)\cdot 1} \ldots \alpha^{(i-1)(N-1)}]$.

One can now write the last expression in an other form by considering A_{i-1} and the differences as inputs of the modified FEQ

$$Z_i^{(k)} = A_{i-1} \cdot \underbrace{\left[1|\alpha^{i-1}|\alpha^{(T-1)(i-1)}\right] \cdot \mathbf{w}_i}_{v_{i,0}} + (b-f) \cdot \underbrace{[0|1|\alpha^{i-1}] \cdot \mathbf{w}_i}_{v_{i,1}} + (c-e) \cdot \underbrace{[0\,0\,1] \cdot \mathbf{w}_i}_{v_{i,2}}. \tag{27}$$

The modified FEQ, i.e., the FEQ with these new inputs, is then found as

$$\begin{bmatrix} v_{i,0} \\ v_{i,1} \\ v_{i,2} \end{bmatrix} = \begin{bmatrix} 1 & \alpha^{i-1} & \alpha^{(T-1)(i-1)} \\ 0 & 1 & \alpha^{i-1} \\ 0 & 0 & 1 \end{bmatrix} \cdot \mathbf{w}_i \tag{28}$$

or similarly

$$[v_{i,0} \quad v_{i,1} \quad v_{i,2}] = \mathcal{F}_4(i,:) \cdot \begin{bmatrix} w_{i,0} & w_{i,1} & w_{i,2} \\ w_{i,1} & w_{i,2} & 0 \\ w_{i,2} & 0 & 0 \\ 0 & 0 & 0 \end{bmatrix}. \tag{29}$$

From

$$\begin{bmatrix} 1 & \alpha^{i-1} & \alpha^{(T-1)(i-1)} \\ 0 & 1 & \alpha^{i-1} \\ 0 & 0 & 1 \end{bmatrix}^{-1} = \begin{bmatrix} 1 & -\alpha^{i-1} & 0 \\ 0 & 1 & -\alpha^{i-1} \\ 0 & 0 & 1 \end{bmatrix}$$

it follows that a simple recursion formula may be obtained, namely

$$v_{i,t+1} \cdot \alpha^{i-1} + w_{i,t} = v_{i,t} \tag{30}$$

for tone $i = 1 \cdots N$ with $t = 0 \cdots T-2$ and $v_{i,T-1} = w_{i,T-1}$. SFGs of the recursion are presented in Fig. 5 for transformation from $\mathbf{v}_i$ to $\mathbf{w}_i$ and vice versa.

ACKNOWLEDGMENT

This work was carried out at the ESAT Laboratory of the Katholieke Universiteit Leuven, in the frame of the Belgian State, Prime Minister's Office—Federal Office for Scientific, Technical and Cultural Affairs—Interuniversity Poles of Attraction Programme IUAP P4-02 (1997–2001): Modeling, Identification, Simulation and Control of Comples Systems. the Concerted Research Action GOA-MEFISTO-666 of the Flemish Government, the IT projects in the ITA-bis program of the Flemish Institute for Scientific and Technological Research in Industry (I.W.T.) (IRMUT (980271) and Advanced Internet Access (980316).

REFERENCES

[1] J. A. C. Bingham, "Multicarrier modulation for data transmission: An idea whose time has come," *IEEE Commun. Mag.*, vol. 28, pp. 5–14, May 1990.

[2] T. Pollet, H. Steendam, and M. Moeneclaey, "Performance degradation of multi-carrier systems caused by an insufficient guard interval duration," in *Proc. Int. Workshop on Copper Wire Access Systems 'Bridging the Last Copper Drop' (CWAS'97)*, pp. 265–270.

[3] N. Al-Dahir and J. M. Cioffi, "Optimum finite-length equalization for multicarrier transceivers," *IEEE Trans. Commun.*, vol. 44, pp. 56–64, Jan. 1996.

[4] I. Lee, J. S. Chow, and J. M. Cioffi, "Performance evaluation of a fast computation algorithm for the DMT in high-speed subscriber loop," *IEEE J. Select. Areas Commun.*, vol. 13, pp. 1564–1570, Dec. 1995.

[5] P. J. W. Melsa, R. C. Younce, and C. E. Rohrs, "Impulse response shortening for discrete multitone transceivers," *IEEE Trans. Commun.*, vol. 44, pp. 1662–1672, Dec. 1996.

[6] M. Van Bladel and M. Moeneclaey, "Time-domain equalization for multicarrier communication," in *Proc. IEEE Global Telecommunications Conf. (Globecom'95)*, pp. 167–171.

[7] J. F. Van Kerckhove and P. Spruyt, "Adapted optimization criterion for FDM-based DMT-ADSL equalization," in *Proc. Int. Communications Conf. (ICC'96)*, pp. 1328–1334.

[8] T. Pollet and M. Peeters, "Synchronization with DMT modulation," *IEEE Commun. Mag.*, vol. 37, pp. 80–86, April 1999.

[9] B. Hirosaki, "An analysis of automatic equalizers for orthogonally multiplexed QAM systems," *IEEE Trans. Commun.*, vol. COM-28, pp. 73–83, Jan. 1980.

[10] B. Hirosaki, S. Hasegawa, and A. Sabato, "Advanced groupband data modem using orthogonally multiplexed QAM technique," *IEEE Trans. Commun.*, vol. COM-34, pp. 587–592, June 1986.

[11] L. Vandendorpe, "Fractionally spaced linear and DF MIMO equalizers for multitone systems without guard time," *Ann. Telecommun.*, vol. 52, no. 1/2, pp. 21–30, Jan.-Feb. 1997.

[12] B. Farhang-Boroujeny and Y. C. Lim, "A comment on the computational complexity of sliding FFT," *IEEE Trans. Circuits Syst.*, vol. 39, pp. 875–876, Dec. 1992.

[13] G. Golub and C. Van Loan, *Matrix Computations*. Baltimore, MD: Johns Hopkins Univ. Press, 1989.

[14] *Network and customers interfaces, asymmetric digital subscriber line (ADSL), metallic interface*, ANSI T1.413-1995.

Katleen Van Acker was born in Reet, Belgium, in 1973. She received the electrical engineering degree from the Katholieke Universiteit Leuven, Leuven, Belgium, in 1996. She is currently working toward the Ph.D. degree in applied sciences at the Electrical Engineering Department of the Katholieke Universiteit Leuven.

Her research interests are in signal processing for digital communications, in particular equalization and echo cancellation for DMT receivers.

Geert Leus was born in Leuven, Belgium, in 1973. He received the electrical engineering degree and the Ph.D. degree in applied sciences from the Katholieke Universiteit Leuven, Leuven, Belgium, in 1996 and 2000, respectively.

Currently, he is a Postdoctoral Fellow of the Fund for Scientific Research—Flanders (FWO-Vlaanderen) at the Electrical Engineering Department of the Katholieke Universiteit Leuven. His research interests are in the area of signal processing for digital communications.

Marc Moonen (M'94) was born in St-Truiden, Belgium, in 1963. He received the electrical engineering degree and the Ph.D. degree in applied sciences from the Katholieke Universiteit Leuven, Leuven, Belgium, in 1986 and 1990, respectively.

Since 1994, he has been a Research Associate with the Belgian NFWO (National Fund for Scientific Research) at the Electrical Engineering Department of the Katholieke Universiteit Leuven. His research activities are in mathematical systems theory and signal processing, parallel computing, and digital communications.

Dr. Moonen received the 1994 K.U. Leuven Research Council Award, the 1997 Alcatel Bell (Belgium) Award (with Piet Vandaele), and was a 1997 "Laureate of the Belgium Royal Academy of Science." He is Chairman of the IEEE Benelux Signal Processing Chapter, a EURASIP officer, and a Member of the Editorial Board of "Integration, the VLSI Journal."

Olivier van de Wiel obtained the degree in electrical engineering from the Université Catholique de Louvain (Belgium).

After finishing his studies he worked in the Communications and Remote Sensing Unit, as a Research Engineer on advanced radio-communications systems, mainly concentrating on DSP for multicarrier and CDMA radio systems. After a short period in the local loop planning cell of the Belgian operator, he joined the Alcatel Telecomm Research Centre, where he was a Systems Engineer on projects concerning ADSL and VDSL. His main interests focus on advanced modulation schemes and equalization techniques. At present, he is Technical Officer at the Secretariat of the European Telecommunication Standard Institute (ETSI), more specifically supporting technical committees involved in the standardization of transmission and access systems.

Thierry Pollet received a diploma degree in electrical engineering from the University of Ghent, Ghent, Belgium, in 1989.

From 1989 to 1996, he was employed at the Communications Engineering Laboratory, University of Ghent, as a Research Assistant. In 1996, he joined the Alcatel Corporate Research Center, Antwerp, Belgium. Currently, he is Project Manager for the Strategic Program Access to Networks. His main interests are high-speed copper transmission, digital communications, equalization, and synchronization.